Polymer Degradation and Stability xxx (2013) 1–14

Contents lists available at ScienceDirect

Polymer Degradation and Stability

journal homepage: www.elsevier.com/locate/polydegstab

Flame-retarded bisphenol A polycarbonate/silicon rubber/bisphenol A bis(diphenyl phosphate): Adding inorganic additives

Eliza Wawrzyn [a], Bernhard Schartel [a,*], Andrea Karrasch [b], Christian Jäger [b]

[a] BAM Federal Institute for Materials Research and Testing, Unter den Eichen 87, 12205 Berlin, Germany
[b] BAM Federal Institute for Materials Research and Testing, Richard-Willstaetter Str. 11, 12489 Berlin, Germany

ARTICLE INFO

Article history:
Received 5 July 2013
Received in revised form
5 August 2013
Accepted 8 August 2013
Available online xxx

Keywords:
Flame retardancy
Polycarbonate blends
Aryl phosphate
Inorganic fillers

ABSTRACT

Various inorganic additives belonging to four different groups: layered materials, metal hydroxides, metal oxides/carbonate and metal borates are investigated in bisphenol A polycarbonate/silicon rubber/bisphenol A bis(diphenyl phosphate) (PC/SiR/BDP) to improve flame retardancy. The pyrolysis, reaction to small flame and fire behaviour of the blends are characterised and structure–property relationships discussed. Among the added layered materials, talc functions as an inert filler with potential for commercialisation, whereas organically modified montmorillonite (LS) enhances decomposition. PC/SiR/BDP + talc and PC/SiR/BDP + LS reinforce the char and induce a flow limit. The different dispersion and location of boehmite (AlO(OH)) nano-particles and $Mg(OH)_2$ micro-particles determine the impact on performance. PC/SiR/BDP + $Mg(OH)_2$ shows additional hydrolysis and thus reduced flame retardancy. AlO(OH) is embedded in SiR and thus behaves as an inert filler. Both additives worked as smoke suppressants. Using selective filling with nano-particles is proposed as an interesting route for flame retardancy in PC/SiR blends. Adding metal oxides and carbonate (MgO, $CaCO_3$ and SiO_2) changes the decomposition pathways of PC/SiR/BDP, worsening the fire performance of PC/SiR/BDP. $CaCO_3$ harbours the potential to intumescence, even though an early collapse of the char structure occurred. Adding hydrated metal borates, CaB, MgB and ZnB, changes the pyrolysis and flame retardancy action. Smoke suppression occurs; LOI is improved as well as UL 94 classification. ZnB performs better than MgB and CaB. The comprehensive study, also based on systematic material variation, delivers valuable guidelines for future development of flame-retarded multi-component PC blends.

1. Introduction

Recently, silicon acrylate rubber (SiR) with high content of polydimethylsiloxane (PDMS) has been proposed as a novel impact modifier for flame-retarded bisphenol A polycarbonate (PC) blends [1,2]. SiR successfully exchanges the easy flammable acrylonitrile-butadiene-styrene (ABS) in a PC/impact modifier blend flame-retarded with bisphenol A bis(diphenyl phosphate) (BDP) and leads to great improvement in LOI of about 10% and to V0 classification in UL 94 [3].

The flame retardancy of BDP in PC blends is based on the gas-phase and condensed-phase modes of action [4–9]. BDP releases phosphorous species which reduce combustion efficiency in the flame (flame poisoning) [10,11]. In the condensed phase BDP reacts with the polymer and induces cross-linking [12–14]. Apart from the advantages due to the replacement of ABS, it was observed that combining PDMS with BDP in the PC/SiR/BDP system worsens the BDP action to some extent, both in the gas phase and in the condensed phase [3]. PDMS reacts with BDP and PC during combustion and leads to a silicon oxide network. The interactions between PDMS, PC and BDP compete with the release of phosphorous species and PC-BDP cross-linking [3,15,16].

Flame retardancy can be improved by adding inorganic fillers [17]. Various inorganic fillers are known for this purpose such as: layered inert materials, metal hydroxides, metal oxides, carbonates and borates. The general flame retardant mechanism of layered materials lies in the creation of a protective layer that limits heat transfer into the material, volatilisation of combustible decomposition products and diffusion of oxygen into the material [18–20]. Inorganic hydroxides work via endothermic decomposition accompanied by the release of water. This affects combustion in several ways, including: cooling, heat sink, diluting the polymer in the condensed and gas phases, decreasing the amount of available fuel, decreasing feedback energy to the pyrolysing polymer and creating a layer of insulation by the oxides remaining in the char [21–24]. Metal oxide fillers interacting with the decomposing

* Corresponding author. Tel.: +49 30 8104 1021.
E-mail address: bernhard.schartel@bam.de (B. Schartel).

0141-3910/$ – see front matter © 2013 Elsevier Ltd. All rights reserved.
http://dx.doi.org/10.1016/j.polymdegradstab.2013.08.006

polymer were reported to improve both the carbonaceous char amount and the mechanical properties of fire residues due to an inorganic carbonaceous structure [25–27]. Silica particles accumulate on the surface of burning materials and generate a high sealing residue that works as a barrier [28–31]. Amorphous spherically shaped silicon dioxide was found to improve flame retardancy and provide good particle distribution [29,31,32]. Carbonates decompose endothermically and liberate CO_2, which dilutes the flammable gases [33]. Metal ions were found to interact with the polymer and form ionomer cross-linking [34,35]. Liberation of CO_2 and ionic interactions led to the formation of intumescent structures [36]. Borates are another family of inorganic additives with flame-retardant properties [37–39]. Among them, zinc borates are the most frequently used. Borates dehydrate endothermically; liberate water, which absorbs the heat and dilutes the fuel in the gas phase; and yield boron oxide (B_2O_3), leading to the formation of a protective vitreous layer [39,40].

The focus of this study is to understand the flame retardancy in PC/SiR/BDP blends when inorganic fillers are added. Various inorganic additives that also disperse differently in PC/SiR/BDP are systematically investigated by selecting the following groups:

1. layered fillers: talc and organically modified layered silicate (LS); generally expected to act as inert materials; talc possesses a microstructure, whereas the LS used forms nanocomposites;
2. metal hydroxides: magnesium hydroxide ($Mg(OH)_2$) and boehmite (AlO(OH)); $Mg(OH)_2$forms a microcomposite and is one of the most often used metal hydroxides, whereas boehmite was applied as nanoparticles to form a nanocomposite;
3. metal oxides and carbonates: magnesium oxide (MgO) and spherically-shaped amorphous silicon dioxide (SiO_2) with different dispersions: micro and nano, respectively, as well as chalk ($CaCO_3$) with a microstructure;
4. metal borates: zinc borate (ZnB), calcium borate (CaB) and magnesium borate (MgB) with different water content and different metals.

This paper addresses the scientific understanding as well as the enhancement of the flame-retardant effects and mechanisms using various inorganic adjuvants in PC/SiR/BDP. The corresponding structure–property relationships are sketched. This study enables the effective selection of the most appropriate inorganic fillers between the limits of the investigated PC/SiR/BDP blends to produce fire-resistant materials.

2. Experimental

Nine different PC/SiR/BDP blends with additional 5 wt.-% inorganic fillers were studied and compared to PC/SiR/BDP. All of the investigated materials contained around 0.6 wt.-% of other additives and 0.45 wt.-% poly(tetrafluoroethylene) (PTFE) as an anti-dripping agent, added as a coagulated 1:1 mixture with styrene-acrylonitrile (SAN). SiR consisted of a PDMS/poly(n-butyl acrylate) (PBA) core surrounded by a poly(methyl methacrylate) (PMMA) shell. Over all the composition of SiR was: 82 wt.-% PDMS, 7 wt.-% PBA and 11 wt.-% PMMA. BDP had an averaged number of repeating units of 1.1 and contained about 2.5% of triphenyl phosphate. PC/SiR/BDP consisted of 71 wt.-% PC, 15 wt.-% SiR and 12.5 wt.-% BDP; after adding the distinct inorganic adjuvants, 66.8 wt.-% PC, 14.2 wt.-% SiR, 12.5 wt.-% BDP and 5 wt.-% inorganic filler. The investigated blends with fillers are classified in four groups: (1) layered inert materials: PC/SiR/BDP + talc, PC/SiR/BDP + LS, (2) metal hydroxides: PC/SiR/BDP + $Mg(OH)_2$, PC/SiR/BDP + AlO(OH), (3) metal oxides: PC/SiR/BDP + MgO, PC/SiR/BDP + SiO_2 and carbonate: PC/SiR/BDP + $CaCO_3$, (4) hydrated metal borates: PC/SiR/BDP + ZnB, PC/SiR/BDP + CaB, PC/SiR/BDP + MgB. The different systems are discussed within their group and compared with PC/SiR/BDP. The following additives were dispersed on the nano-scale: LS and AlO(OH), whereas talc, $Mg(OH)_2$, MgO, $CaCO_3$ and borates formed microcomposites. The special SiO_2 used was dispersed very well into single particles. Thus PC/SiR/BDP + SiO_2 was between a nanocomposite and a microcomposite, with each single particle smaller and larger than 100 nm in size. The layered silicate was organically modified by exchanging the sodium with stearyl benzyl dimethyl ammonium to achieve good dispersion within PC/SiR/BDP. The SiO_2 was mixed with PC/SiR/BDP as Sidistar T120 XP. The Sidistar T120 XP is an amorphous spherically-shaped silicon dioxide with an average primary particle size of 150 nm and a broad particle size distribution of between 20 and 500 nm. The following borates were used: zinc borate with a molecular formula of $2ZnO \cdot 3B_2O_3 \cdot 3.5H_2O$ (here called ZnB, known in the trade as Firebrake ZB) which contains around 13.5 wt.-% of water, calcium borate $CaO \cdot 2B_2O_3 \cdot 3.5H_2O$ (called CaB) with the highest water content of around 24.0 wt.-%, and magnesium borate $MgO \cdot B_2O_3 \cdot 1.5H_2O$ (called MgB) with around 19.0 wt.-% of water. All the blends were provided by BayerMaterial Science AG (Dormagen, Germany) as granulate, bars and plates.

Thermogravimetry (TG) was performed with a TGA/SDTA 851 (Mettler Toledo, Germany) under nitrogen flow of 30 ml min^{-1}. Samples of 15 mg were investigated with a heating rate of 10 K min^{-1} in alumina pans from room temperature up to about 1200 K. The decomposition kinetics was evaluated based on using different heating rates (2, 5, 10 and 20 K min^{-1}) and 10 mg samples. The activation energy was determined by the method of Ozawa-Flynn-Wall [41]. The same TG apparatus coupled with a Fourier transform infrared spectrometer Nexus 470 (Nicolet, Germany) (TG-FTIR) was applied to analyse the evolved gases. The coupling transfer tube (inner diameter of 1 mm) was heated to 473 K; the infrared cell to 483 K.

Cone calorimeter (FTT, UK) tests were performed following ISO 5660 to investigate the fire behaviour under forced flaming conditions. Three irradiations were used, 35, 50 and 70 kW m^{-2}. The specimens (100 mm × 100 mm × 4 mm) were measured horizontally using the frame. The calculations were based on the reduced area of 88.36 cm^2 instead of 100 cm^2. The UL 94 test according to IEC 60695-11-10 and the oxygen index (LOI) following ISO 4589 were used to characterise the reaction to a small flame. The specimens were preconditioned (ISO 219, 296 K, 50% r.h.) for 88 h before fire testing. The LOI specimens were 80 mm × 10 mm × 4 mm. Two thicknesses were tested in the UL 94: 120 mm × 12.5 mm × 1.6 mm and 120 mm × 12.5 mm × 3.2 mm. The fire residues of PC/SiR/BDP, PC/SiR/BDP + $CaCO_3$ and PC/SiR/BDP + SiO_2 were characterised by scanning electron microscopy SEM (FEI XL30 ESEM, Eindhoven, the Netherlands) after sputtering with thin layers of gold [42]. An energy-dispersive X-ray microanalysis system (EDX-SEM) was used to monitor the element distribution in the fire residue of PC/SiR/BDP + SiO_2.

Solid state ^{31}P and ^{29}Si MAS NMR of PC/SiR/BDP and PC/SiR/BDP + ZnB were performed with a DMX 400 spectrometer (Bruker Biospin GmbH, Rheinstetten, Germany). The measurements were carried out at room temperature. For ^{31}P MAS NMR experiments, a 90° pulse length of 3.7 μs and a repetition time of 600 s were used; 64 scans were accumulated. For ^{29}Si MAS NMR experiments a 90° pulse length of 6 μs was used. The repetition rate was 180 s and 256 scans were accumulated. ^{11}B rs echo MAS NMR experiments on PC/SiR/BDP + ZnB were performed using a Bruker Avance 600 spectrometer. The selective π/2 pulse length was 2.5 μs and 256 scans were accumulated. The repetition time was 120 s. The background signal (boron nitride stator) was eliminated by the measurement of an empty rotor under identical

Please cite this article in press as: Wawrzyn E, et al., Flame-retarded bisphenol A polycarbonate/silicon rubber/bisphenol A bis(diphenyl phosphate): Adding inorganic additives, Polymer Degradation and Stability (2013), http://dx.doi.org/10.1016/j.polymdegradstab.2013.08.006

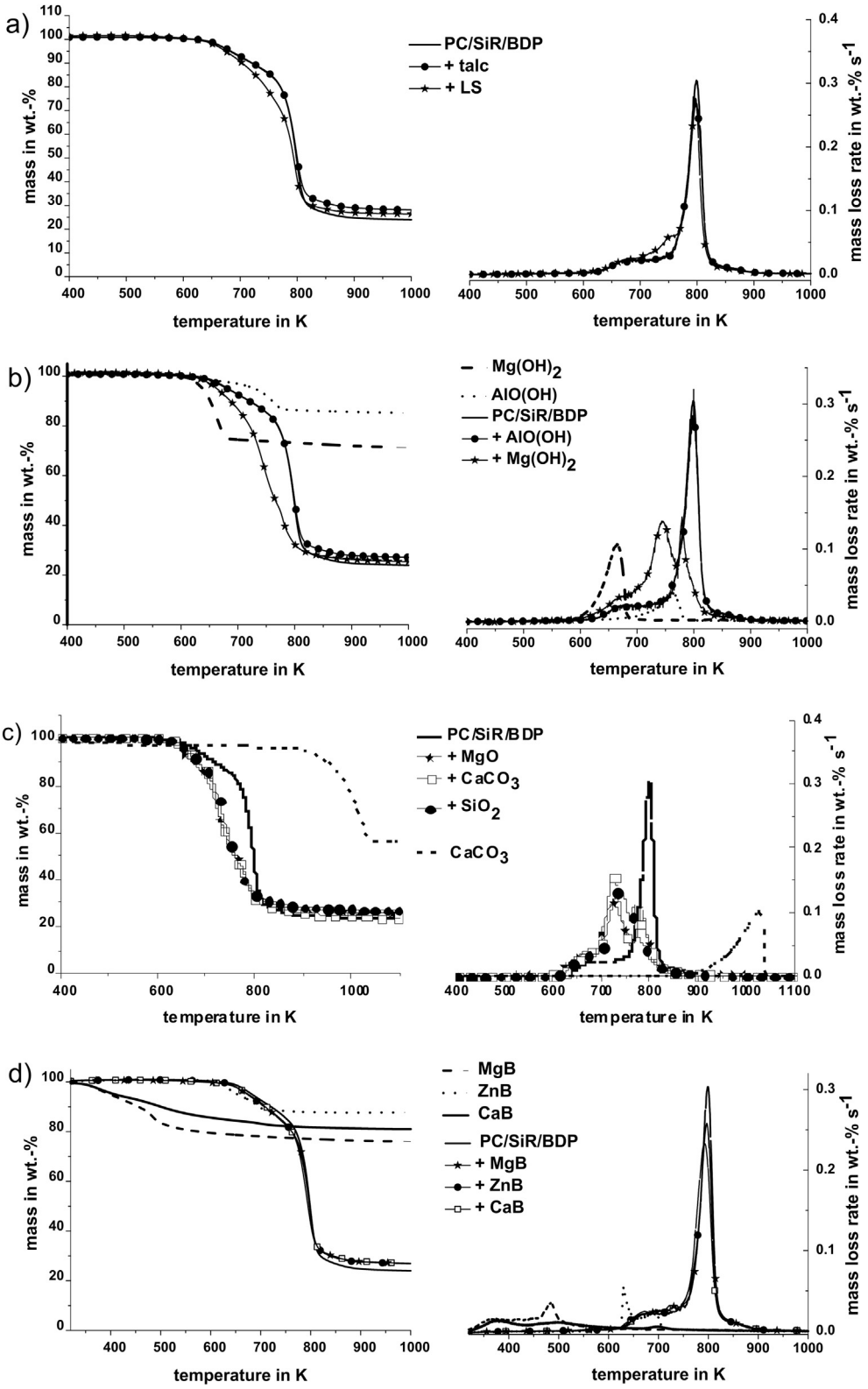

Fig. 1. Mass and mass loss rate (thermogravimetry under N_2, heating rate 10 K min^{-1}): a) PC/SiR/BDP, PC/SiR/BDP + talc and PC/SiR/BDP + LS; b) PC/SiR/BDP, PC/SiR/BDP + $Mg(OH)_2$, PC/SiR/BDP + AlO(OH), $Mg(OH)_2$, and AlO(OH); c) PC/SiR/BDP, PC/SiR/BDP + MgO, PC/SiR/BDP + SiO_2, PC/SiR/BDP + $CaCO_3$ and $CaCO_3$; d) PC/SiR/BDP, PC/SiR/BDP + ZnB, PC/SiR/BDP + CaB, PC/SiR/BDP + MgB, ZnB, CaB and MgB.

conditions. The resulting background NMR spectrum was subtracted from the NMR spectra of PC/SiR/BDP + ZnB. Representative residues were prepared in a quartz tube furnace with an inner diameter of 38 mm and length of 40 cm under a N_2 flow of 100 ml min^{-1}. Powder was placed in a quartz boat and heated up to set-point temperature (between 630 K and 850 K) at a heating rate of 10 K min^{-1}. After 30 min at the set-point temperature the residues were cooled down.

Please cite this article in press as: Wawrzyn E, et al., Flame-retarded bisphenol A polycarbonate/silicon rubber/bisphenol A bis(diphenyl phosphate): Adding inorganic additives, Polymer Degradation and Stability (2013), http://dx.doi.org/10.1016/j.polymdegradstab.2013.08.006

Table 1
Thermogravimetry (TG) under N_2, heating rate 10 K min^{-1}: Part 1) PC/SiR/BDP PC/SiR/BDP + talc, PC/SiR/BDP + LS, PC/SiR/BDP + $Mg(OH)_2$, and PC/SiR/BDP + AlO(OH); Part 2) PC/SiR/BDP, PC/SiR/BDP + MgO, PC/SiR/BDP + SiO_2, PC/SiR/BDP + $CaCO_3$, PC/SiR/BDP + ZnB, PC/SiR/BDP + CaB and PC/SiR/BDP + MgB.

Part 1	PC/SiR/BDP	+talc	+LS	+$Mg(OH)_2$	+AlO(OH)
$T_{2wt.-\%}$ ± 2/K	647	645	635	631	648
1st mass loss (PMMA and PBA decomposition of SiR)					
T_{max} ± 2/K	676	676	676	674	676
Weight loss ± 1.0/wt.-%	16.5	17.0	11.0	11.5	18.0
2nd mass loss (PDMS + LS; hydrolysis of PC + $Mg(OH)_2$)					
T_{max} ± 2/K	–	–	754	745	
Weight loss ± 1.0/wt.-%	–	–	16.2	42.5	
3rd mass loss (main decomposition step)					
T_{max} ± 2/K	799	799	798	779	799
Weight loss ± 1.0/wt.-%	60.0	47.5	47.5	21.0	54.0
4th mass loss (PDMS decomposition)					
T_{max}/ ± 2 K	–	–	–	–	–
Weight loss ± 1.0/wt.-%	–	–	–	–	–
Residue at 1000 K					
Mass ± 1.0/wt.-%	23.5	28.5	25.3	25.0	28.0

Part 2	PC/SiR/BDP	+MgO	+SiO_2	+$CaCO_3$	+ZnB	+MgB	+CaB
$T_{2wt.-\%}$ ± 2/K	647	616	635	636	642	641	641
1st mass loss (PMMA and PBA decomposition of SiR)							
T_{max} ± 2/K	676	656	663	670	674	675	675
Weight loss ± 1.0/wt.-%	16.5	13.0	12.5	12.0	18.0	18.5	18.0
2nd mass loss (PDMS + LS; hydrolysis of PC + $Mg(OH)_2$)							
T_{max} ± 2/K	–						
Weight loss ± 1.0/wt.-%	–						
3rd mass loss (main decomposition step)							
T_{max} ± 2/K	799	728	741	726	797	799	788
Weight loss ± 1.0/wt.-%	60.0	34.0	39.3	39.0	55.5	53.5	56.0
4th mass loss (PDMS decomposition)							
T_{max}/ ± 2 K	–	782	771	784	–	–	–
Weight loss ± 1.0/wt.-%	–	27.0	21.7	21.0	–	–	–
Residue at 1000 K							
Mass ± 1.0/wt.-%	23.5	26.0	28.5	24.0	26.5	27.4	26.0

The melts were studied by a rheometer (Anton Paar Physica MCR 301) with plate–plate geometry (gap of 1 mm, plate diameter of 25 mm) under nitrogen. Isothermal measurements were conducted in the frequency sweep mode (100 Hz – 0.1 Hz) at 488 K, 498 K, 543 K and 588 K while applying a small deformation (gamma = 0.5%). Master-curves were calculated with the reference temperature of 498 K.

3. Results and discussion

Results of the thermal analysis are presented in Fig. 1 and Table 1 for the investigated PC/SiR/BDP blends with and without inorganic filers. The temperature when 2 wt.-% mass loss was reached ($T_{2wt.-\%}$) is used to describe the beginning of the decomposition, the temperatures when the maxima in mass loss rate occur (T_{max}) are used as characteristic decomposition temperatures. The fire behaviour (different forced-flaming conditions in the cone calorimeter) and flammability (reaction to small flame in the LOI and UL 94 test) results are summarised in Table 2.

The pyrolysis and fire behaviour of PC/SiR/BDP was discussed comprehensively in a previous paper [3]. The first decomposition step was related to PMMA and PBA and the second to PC, PDMS and BDP taking into account the decomposition temperatures, the mass losses, the volatile pyrolysis products and the residue analysis. During pyrolysis PC, PDMS and BDP partially reacted with each other. The pyrolysis residue consisted of graphite-like structures, a silicon dioxide network and inorganic phosphates. The heat release rate (HRR) pattern of PC/SiR/BDP in the cone calorimeter is typical for charring. The maximum HRR (pHRR) was observed right at the beginning of burning, followed by a decreasing HRR due to the formation of the char. The specimen showed a large deformation

Table 2
Cone calorimeter, LOI and UL 94 results. Part 1) PC/SiR/BDP PC/SiR/BDP + talc, PC/SiR/BDP + LS, PC/SiR/BDP + $Mg(OH)_2$, and PC/SiR/BDP + AlO(OH); Part 2) PC/SiR/BDP, PC/SiR/BDP + MgO, PC/SiR/BDP + SiO_2, PC/SiR/BDP + $CaCO_3$, PC/SiR/BDP + ZnB, PC/SiR/BDP + CaB and PC/SiR/BDP + MgB (t_{ig} = time to ignition, pHRR = peak heat release rate, THE = total heat evolved, ML = mass loss, TCOP = total CO production, TSR = total smoke production).

Part 1	PC/SiR/BDP	+talc	+LS	+$Mg(OH)_2$	+AlO(OH)
Cone calorimeter (35 kW m^{-2})					
t_{ig} ± 43/s	160	132	93	258	98
pHRR ± 17/kW m^{-2}	200	179	177	208	202
THE ± 3/MJ m^{-2}	57	57	60	59	61
Residue ± 3.5/wt.-%	30.2	30.0	22.7	29.3	30.0
THE/ML ± 0.1/MJ g^{-1} m^{-2}	2.3	2.3	2.2	2.3	2.4
TCOP/ML ± 0.01/gg^{-1}	0.07	0.09	0.07	0.05	0.08
TSR/ML ± 7/gg^{-1}	98	92	110	91	82
Cone calorimeter (50 kW ± m^{-2})					
t_{ig} ± 25/s	44	44	41	56	96
pHRR ± 28/kW m^{-2}	279	210	218	219	225
THE ± 3/MJ m^{-2}	59	58	57	62	58
Residue ± 2.2/wt.-%	22.0	30.5	23.4	22.6	26.2
THE/ML ± 0.1/MJ g^{-1} m^{-2}	2.2	2.3	2.1	2.2	2.2
TCOP/ML ± 0.01/gg^{-1}	0.08	0.07	0.07	0.07	0.06
TSR/ML ± 9/gg^{-1}	106	92	123	100	92
Cone calorimeter (70 kW m^{-2})					
t_{ig} ± 3/s	25	24	21	29	30
pHRR ± 15/kW m^{-2}	274	252	242	253	243
THE ± 3/MJ m^{-2}	52	58	51	58	59
Residue ± 2.7/wt.-%	26.2	28.5	23.2	24.9	27.9
THE/ML ± 0.1/MJ g^{-1} m^{-2}	2.0	2.2	1.9	2.1	2.2
TCOP/ML ± 0.01/gg^{-1}	0.07	0.06	0.07	0.05	0.06
TSR/ML ± 10/gg^{-1}	128	104	130	115	96
Flammability					
LOI ± 1/%	37.6	29.7	29.2	34.8	34.4
UL 94 (3.2 mm)	V0	V0	V0	V0	V0
UL 94 (1.6 mm)	V0	V0	V0	HB	V0	V0

Part 2	PC/SiR/BDP	+MgO	+SiO_2	+$CaCO_3$	+ZnB	+MgB	+CaB
Cone calorimeter (35 kW m^{-2})							
t_{ig} ± 43/s	160	94	104	142	174	137	124
pHRR ± 17/kW m^{-2}	200	208	228	210	217	208	205
THE ± 3/MJ m^{-2}	57	64	62	61	59	59	57
Residue ± 3.5/wt.-%	30.2	26.2	26.3	27.2	31.6	30.4	30.4
THE/ML ± 0.1/MJ g^{-1} m^{-2}	2.3	2.4	2.3	2.3	2.4	2.3	2.3
TCOP/ML ± 0.01/gg^{-1}	0.07	0.04	0.06	0.03	0.05	0.06	0.06
TSR/ML ± 7/gg^{-1}	98	103	98	94	83	96	98
Cone calorimeter (50 kW m^{-2})							
t_{ig} ± 25/s	44	49	44	66	38	43	66
pHRR ± 28/kW m^{-2}	279	240	260	273	218	251	211
THE ± 3/MJ m^{-2}	59	61	61	60	61	58	57
Residue±2.2/wt.-%	22.0	27.4	22.4	24.6	28.8	24.4	27.2
THE/ML ± 0.1/MJ g^{-1} m^{-2}	2.2	2.3	2.2	2.2	2.4	2.1	2.2
TCOP/ML ± 0.01/gg^{-1}	0.08	0.04	0.07	0.04	0.05	0.06	0.06
TSR/ML ± 9/gg^{-1}	106	114	110	112	86	109	99
Cone calorimeter (70 kW m^{-2})							
t_{ig} ± 3/s	25	21	23	34	18	20	24
pHRR ± 15/kW m^{-2}	274	293	275	276	264	257	252
THE ± 3/MJ m^{-2}	52	57	58	54	55	57	52
Residue ± 2.7/wt.-%	26.2	26.0	24.0	24.8	29.8	26.5	28.7
THE/ML ± 0.1/MJ g^{-1} m^{-2}	2.0	2.1	2.1	2.0	2.2	2.3	2.1
TCOP/ML ± 0.01/gg^{-1}	0.07	0.05	0.06	0.04	0.05	0.06	0.06
TSR/ML ± 10/gg^{-1}	128	126	118	121	102	120	108
Flammability							
LOI ± 1/%	37.6	31.4	31.1	29.6	37.9	38.3	38.9
UL 94 (3.2 mm)	V0	V1	V0	HB	V0	V0	V0
UL 94 (1.6 mm)	V0	V1	V0	HB	V0	V0	V0

Please cite this article in press as: Wawrzyn E, et al., Flame-retarded bisphenol A polycarbonate/silicon rubber/bisphenol A bis(diphenyl phosphate): Adding inorganic additives, Polymer Degradation and Stability (2013), http://dx.doi.org/10.1016/j.polymdegradstab.2013.08.006

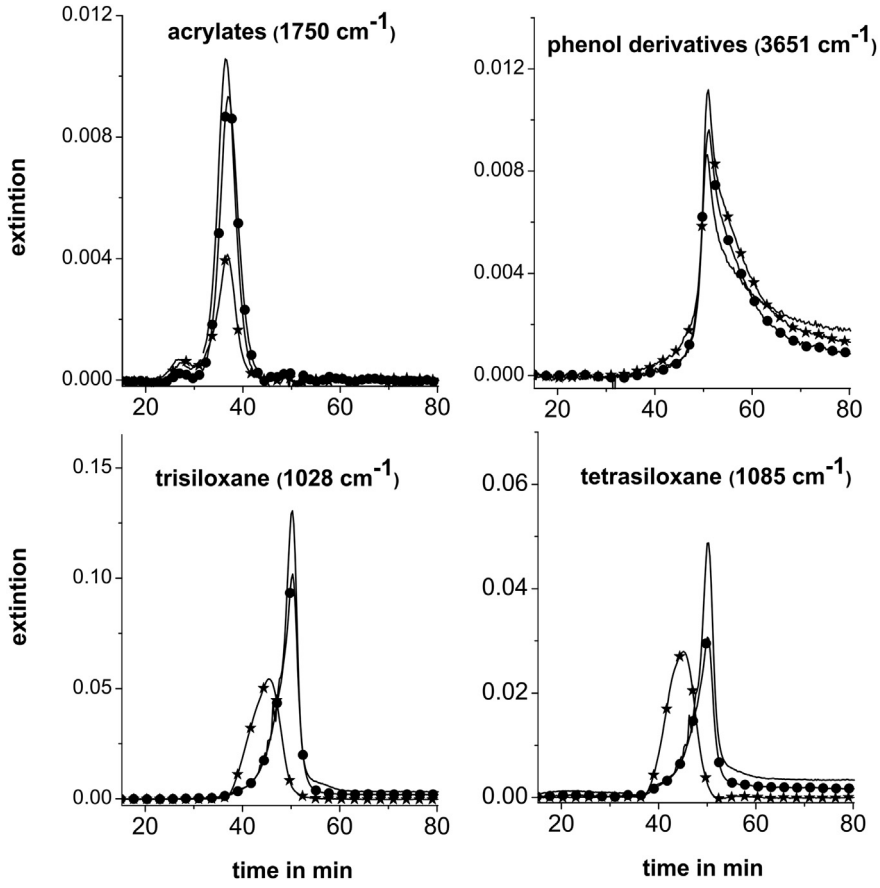

Fig. 2. Pyrolysis product release rates (TG-FTIR) for PC/SiR/BDP (line), PC/SiR/BDP + talc (circles), and PC/SiR/BDP + LS (stars).

starting from the 3 mm thick plate and ending up with a several centimetres high char tower. A second, smaller pHRR occurred at the end of combustion, which was attributed to char decomposition [43]. The interactions between PC, PDMS and BDP were found to reduce the BDP gas-phase and condensed-phase action to some extent.

3.1. Layered inert fillers

PC/SiR/BDP + talc started to decompose at the same temperature as PC/SiR/BDP (Fig. 1a, Table 1) and showed the same two-steps decomposition. Only the residue was increased and the mass loss decreased by 5 wt.-%, respectively, demonstrating the inert filler characteristic of talc in PC/SiR/BDP. PC/SiR/BDP + LS began to decompose 12 K before PC/SiR/BDP ($T_{2wt.-\%}$ characterises the beginning of decomposition), and three decomposition processes were observed. An additional shoulder (2nd mass loss) appeared before the main step. The decomposition temperatures (maxima in mass loss rate) for the first and the main decomposition steps were unchanged in comparison to PC/SiR/BDP. The residue of PC/SiR/BDP + LS was lower than what was expected from a superposition of the residues of PC/SiR/BDP and 5 wt.-% of LS, indicating an additional interaction between the components.

The volatile pyrolysis products were identified by product-specific peaks in FTIR; the release rates by following the intensity of the characteristic peaks. The decomposition of PMMA and PBA resulted in peaks at 1750 cm^{-1} coming from the carbonyl group (C═O), the decomposition of BDP at 960 cm^{-1} from P–O-aryl vibration, the decomposition of PC at 2361 cm^{-1} from CO_2 and at 3015 cm^{-1} from CH_4 as well as at 3651 cm^{-1} from phenol derivatives (aryl-OH), and the decomposition of PDMS at 1028 cm^{-1} from hexamethylcyclotrisiloxane and at 1085 cm^{-1} from octamethylcyclotetrasiloxane. PC/SiR/BDP + talc released a slightly lower amount of pyrolysis products at the same time as PC/SiR/BDP (Fig. 2). At the first decomposition step (~36 min) the acrylic components evolved, whereas at the main step (~50 min) carbon dioxide, methane, phenol derivatives, tri- and tetrasiloxanes did. Further, the activation energy versus conversion (Fig. 3) indicated the same reaction kinetics for PC/SiR/BDP and PC/SiR/BDP + talc. Two decomposition processes were indicated by two different activation energies. The first process with the lower activation

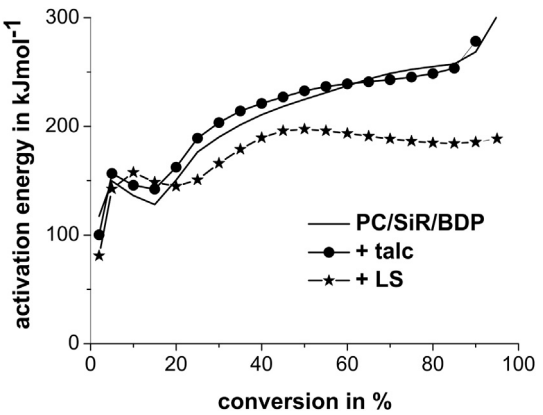

Fig. 3. Activation energy (E_A) versus conversion, comparing PC/SiR/BDP, PC/SiR/BDP + talc and PC/SiR/BDP + LS.

Please cite this article in press as: Wawrzyn E, et al., Flame-retarded bisphenol A polycarbonate/silicon rubber/bisphenol A bis(diphenyl phosphate): Adding inorganic additives, Polymer Degradation and Stability (2013), http://dx.doi.org/10.1016/j.polymdegradstab.2013.08.006

energy occurred below 20% and thus corresponded well to the first mass loss in TG.

For PC/SiR/BDP + LS acrylic components and phenol derivatives were released at the same time as PC/SiR/BDP (Fig. 2), whereas tri- and tetrasiloxanes were released earlier. The maximum of siloxane release at around 45 min for PC/SiR/BDP + LS corresponds well to the second mass loss at 754 K. The release of acrylates was clearly reduced for PC/SiR/BDP + LS compared to PC/SiR/BDP. Apart from siloxanes, the rates of decomposition of other products were also slightly reduced. Further, the activation energy pattern of PC/SiR/BDP + LS differed from that of PC/SiR/BDP (Fig. 3). A minimum appeared at 20% conversion rather than below. This broader first decomposition process most probably indicated enhanced interaction between acrylic components and PC, which may explain the reduced acrylate release. The last process corresponded to the decomposition of PC and showed a lowered value for PC/SiR/BDP + LS, when compared with PC/SiR/BDP.

With respect to pyrolysis, talc functions as an inert filler. There was no difference in mass loss and mass loss rate between PC/SiR/BDP + talc and PC/SiR/BDP. The reaction kinetics was also very similar for these blends. The release rates of decomposition gases were only slightly lower due to the dilution of the polymer through the addition of talc. LS in PC/SiR/BDP + LS is chemically active during pyrolysis. The decomposition occurred at lower temperatures. The facilitation of decomposition may be due to catalysis by acidic sites created through the thermal decomposition of the silicate modifier [44]. These acidic sites, combined with the hydroxyl groups of clay, were proposed to yield the lower thermal stability of PDMS in PC/SiR/BDP + LS. Further, adding LS to PC/SiR/BDP reduced carbonaceous char formation. In the presence of LS, PC decomposed more via chain scission, and less rearrangement and cross-linking occurred. The cross-linking between PC and BDP was depleted and BDP cross-linked with PDMS, which decomposed earlier.

Addition of talc and clay to PC/SiR/BDP worsens the LOI by around 8%, from 37.6% to below 30%. Nevertheless the UL 94 classification of PC/SiR/BDP + talc remained V0 for both sample thicknesses (1.6 and 3.2 mm). PC/SiR/BDP + LS achieved V0 only for the 3.2 mm-thick specimen and HB for 1.6 mm. Similar rather disappointing results in flammability for polymer nanocomposites have been reported before for LOI and UL 94 [45,46]. It was concluded that the improved protection layer plays a minor role in tests applying low external heat fluxes [19,20], whereas the typical major changes in melt viscosity often deteriorate LOI and UL 94 crucially in thermoplastics [20,46,47], so that the benefit of the protection layer improvement is counterbalanced or even overruled.

For both PC/SiR/BDP + talc and PC/SiR/BDP + LS, such enhanced changes in rheological performance were observed compared to PC/SiR/BDP (Fig. 4). For all three materials (PC/SiR/BDP + talc, PC/SiR/BDP + LS and PC/SiR/BDP) the logarithm of the shear stress was no longer decreasing linearly with decreasing logarithm of angular frequency, but levels off to a rather constant value for lower frequencies. The dependency on the frequency or shear rate, respectively, was changing from a liquid-like to a solid-like behaviour; thus the materials showed a flow limit, which reduces melt flow and prevent dripping in the LOI and UL 94 tests. PC/SiR/BDP + talc and PC/SiR/BDP + LS showed a much more pronounced flow limit compared to PC/SiR/BDP. Additionally LS functioned as a plasticizer at high shear rates, enabling easier compounding and injection moulding.

The basic HRR patterns of PC/SiR/BDP, PC/SiR/BDP + talc, and PC/SiR/BDP + LS were very similar. All blends were charring and showed a large deformation of the specimen starting from the 3 mm thick plate and ending up with a several centimetres high char tower. They showed an initial increase in HRR until an efficient char layer was formed. Afterwards HRR decreased with increasing

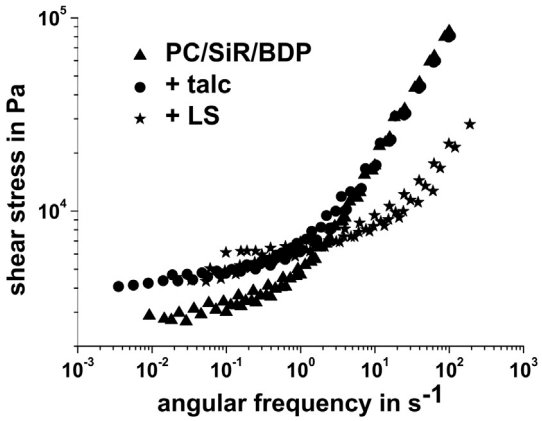

Fig. 4. Shear stress versus angular frequency for PC/SiR/BDP, PC/SiR/BDP + talc and PC/SiR/BDP + LS.

char layer thickness. Both PC/SiR/BDP + talc and PC/SiR/BDP + LS showed a lower maximum in HRR (peak HRR = pHRR) than PC/SiR/BDP due to improved protection properties of the char. Further, PC/SiR/BDP + talc achieved longer burning times and shifted char decomposition to later times. Thus talc improves the stability of the residual char in PC/SiR/BDP + talc. The fire load was hardly changed, the time to ignition was reduced to some extent and the combustion in the gas phase remained nearly unchanged, as has been reported for similar systems before [48].

Both talc and organically modified layered silicate in PC/SiR/BDP worked as a protection layer against heat transport from the flame to the material due to enhanced char properties. However, the protection layer formed on the burning samples of PC/SiR/BDP + talc and PC/SiR/BDP + LS in LOI test was not effective enough to stop the flame so that the sample continues to burn slowly, ultimately displaying worse flammability performance than PC/SiR/BDP.

3.2. Metal hydroxides

The thermal decomposition of the blends PC/SiR/BDP + AlO(OH) and PC/SiR/BDP + $Mg(OH)_2$ are discussed and compared to the decomposition of boehmite and $Mg(OH)_2$ as well as of PC/SiR/BDP (Fig. 1b, Table 1). Decomposition of both AlO(OH) (T_{max} = 761 K) and $Mg(OH)_2$, (T_{max} = 665 K) occurred in a single step. The $Mg(OH)_2$ started decomposition 55 K earlier than AlO(OH). The decomposition process of the hydroxides is attributed to the endothermic release of water that accompanies the formation of metal oxides in the condensed phase. Boehmite loses around 15 wt.-% water vapour and $Mg(OH)_2$ around 29 wt.-%. The mass loss corresponded to the theoretical ones of 15 wt.-% for the reaction to Al_2O_3 + water and 31 wt.-% for the reaction to MgO + water, respectively.

The pyrolysis of PC/SiR/BDP + AlO(OH) was very similar to that of PC/SiR/BDP. PC/SiR/BDP + AlO(OH) started to decompose at the same temperature, and in the same two steps. Hardly any difference was observed (Fig. 1b) apart from the additional 4.5 wt.-% residue and the reduced mass loss, respectively. The additional residue corresponded well to the expected formation of 4.25 wt.-% aluminium oxide resulting from the addition of 5 wt.-% AlO(OH). Incorporation of $Mg(OH)_2$ in PC/SiR/BDP + $Mg(OH)_2$ changed the decomposition. Decomposition began 16 K earlier and three decomposition steps were observed. The T_{max} of the first decomposition step was unchanged in comparison to PC/SiR/BDP, but the main and the last decomposition steps were shifted to significantly lower temperatures. Furthermore, the PC/SiR/BDP + $Mg(OH)_2$ yielded a lower amount of residue (−2 wt.-%) than was expected

Please cite this article in press as: Wawrzyn E, et al., Flame-retarded bisphenol A polycarbonate/silicon rubber/bisphenol A bis(diphenyl phosphate): Adding inorganic additives, Polymer Degradation and Stability (2013), http://dx.doi.org/10.1016/j.polymdegradstab.2013.08.006

from superposition of the PC/SiR/BDP and calculated magnesia (MgO) residue (3.46 wt.-% resulting from adding of 5 wt.-% $Mg(OH)_2$). This indicates less charring of PC and/or less cross-linking between PC and BDP.

PC/SiR/BDP + AlO(OH) released the pyrolysis products at the same time as PC/SiR/BDP. Similar amounts of methane and phenol derivatives (Fig. 5) were observed and slightly lower amounts of acrylate, carbon dioxide and siloxanes. For both blends the acrylic components were evolved at first decomposition step (~36 min), whereas carbon dioxide, methane, phenol derivatives, tri- and tetrasiloxanes appeared during the main step (~ 50 min). The activation energy proves that the reaction kinetics of both blends, PC/SiR/BDP + AlO(OH) and PC/SiR/BDP, were very similar as a function of conversion (Fig. 6). Two decomposition processes were observed indicated by two different activation energies, which was consistent with the results from mass loss and products released.

The product release rates of PC/SiR/BDP + $Mg(OH)_2$ (Fig. 5) show an earlier release for CO_2, phenol derivatives and siloxanes compared to PC/SiR/BDP, whereas acrylates and CH_4 were released at the same time. Thus at the first decomposition step acrylic components of SiR decomposed, the main decomposition step belonged to the decomposition of PC, and the last one to PDMS. Much more phenol derivatives and cyclic siloxanes were released for the system with $Mg(OH)_2$, which means that water supported PDMS, PC and/or BDP chain scission, resulting in less char. The activation energy pattern of PC/SiR/BDP + $Mg(OH)_2$ differed from that for PC/SiR/BDP (Fig. 6). $Mg(OH)_2$ significantly decreased the activation energy of PC/SiR/BDP. At least three processes occurred for PC/SiR/BDP + $Mg(OH)_2$: the first, below 20% of conversion, showed the decomposition of $Mg(OH)_2$ and acrylates from SiR, the second the decomposition of PC, and the last process around 70% conversion was attributed to PDMS decomposition and had the highest activation energy.

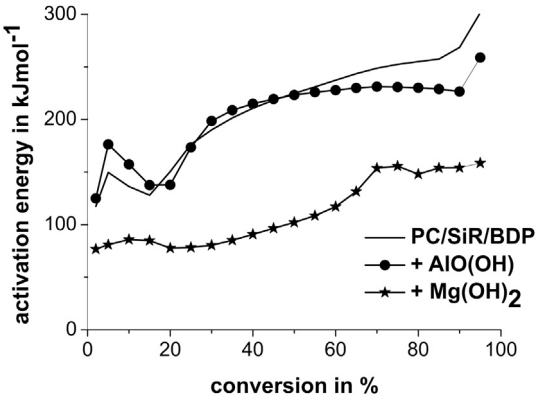

Fig. 6. Activation energy (E_A) versus conversion, comparing PC/SiR/BDP, PC/SiR/BDP + AlO(OH) and PC/SiR/BDP + $Mg(OH)_2$.

With respect to thermal decomposition boehmite functioned as inert filler with no difference in mass loss and mass loss rate between PC/SiR/BDP + AlO(OH) and PC/SiR/BDP. Reaction kinetics was similar and only slightly less acrylates, CO_2 and cyclic siloxanes were released. AlO(OH) particles acted only in a physical way slightly hindering the release of pyrolysis gases. Despite the loss of water from boehmite taking place within the temperature range for PC decomposition, no hydrolysis effect is detected. For PC/SiR/BDP + $Mg(OH)_2$ decomposition occurred at a lower temperature.

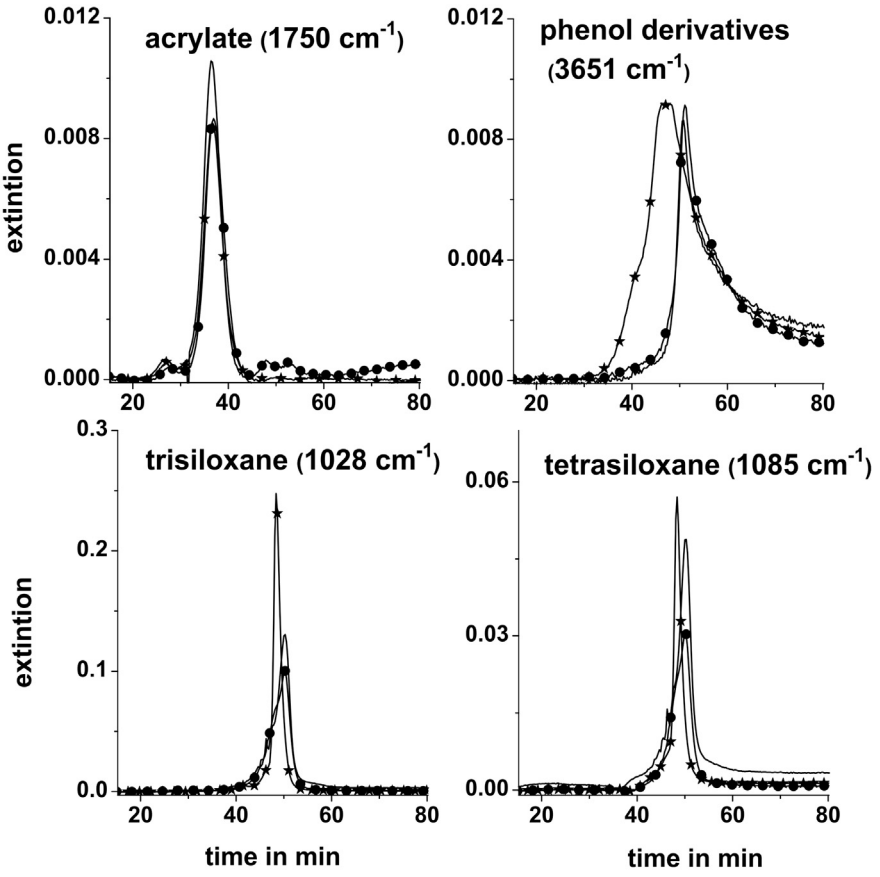

Fig. 5. Pyrolysis product release rates determined by TG-FTIR for PC/SiR/BDP + AlO(OH) (circles) and PC/SiR/BDP + $Mg(OH)_2$ (stars) compared to PC/SiR/BDP (line).

Please cite this article in press as: Wawrzyn E, et al., Flame-retarded bisphenol A polycarbonate/silicon rubber/bisphenol A bis(diphenyl phosphate): Adding inorganic additives, Polymer Degradation and Stability (2013), http://dx.doi.org/10.1016/j.polymdegradstab.2013.08.006

The beginning of decomposition of PC/SiR/BDP + $Mg(OH)_2$ was caused by the release of water. Hydrolysis of the polymers PC, PDMS, and BDP resulted in different decomposition pathways. The reaction between BDP and $Mg(OH)_2$ led to the formation of magnesium phosphates ($Mg_3(PO_4)_2$ and $Mg_2P_2O_7$) [46]. The cross-linking between Fries rearrangement products of PC and phenolic groups of BDP was reduced and thus charring. The formed MgO improved the char structure, hindering the release of small decomposition products like CO_2 and CH_4.

The question arises as to why the AlO(OH) did not cause hydrolysis and $Mg(OH)_2$ did. Three reasons are proposed: the lower water content of AlO(OH), the higher decomposition temperature of boehmite, and the smaller contact area between AlO(OH) and PC despite their finer dispersion. TEM investigations (Fig. 7) revealed the distribution of the inorganic additives in PC/SiR/BDP. Most boehmite particles were coated with PDMS of SiR, preventing PC hydrolysis. Water was released when the main part of PC was already gone. $Mg(OH)_2$ was dispersed in the PC phase, thus liberation of water triggered the hydrolysis of PC.

AlO(OH) and $Mg(OH)_2$ in PC/SiR/BDP showed deterioration (Δ LOI = - 3%) in LOI (Table 2). The UL 94 classifications were unaffected upon incorporation. For both thicknesses (1.6 and 3.2 mm) the V0 class remained.

The HRR patterns of PC/SiR/BDP + AlO(OH), PC/SiR/BDP + $Mg(OH)_2$ and PC/SiR/BDP were similar and typical for charring materials with a second peak HRR at the end of burning attributed to char decomposition. Time to ignition increased for $Mg(OH)_2$ and decreased for AlO(OH), the pHRR were reduced for 50 and 70 kW m^{-2} irradiation. The THE and the residue were hardly changed due to the limited amount of metal hydrate (5 wt.-%) used and most probably due to the compensation by additional hydrolysis of PC decreasing the residue amount. Nevertheless the amount of residue tended to show the order PC/SiR/BDP + $Mg(OH)_2 \leq$ PC/SiR/BDP < PC/SiR/BDP + AlO(OH) that correspond to the thermal analysis. Apart from hydrolysis in the condensed phase, the released amount of water was too small to result in any significant reduction in THE. Far from it, THE was increased for 70 kW m^{-2} irradiation. The increase in time to ignition is typical for metal hydrates and worth noting along with the smoke suppression observed for both fillers.

The fire behaviour of PC/SiR/BDP + AlO(OH) and PC/SiR/BDP + $Mg(OH)_2$ was not improved in more fully developed fires, since the reduced pHRR was compensated by antagonistic

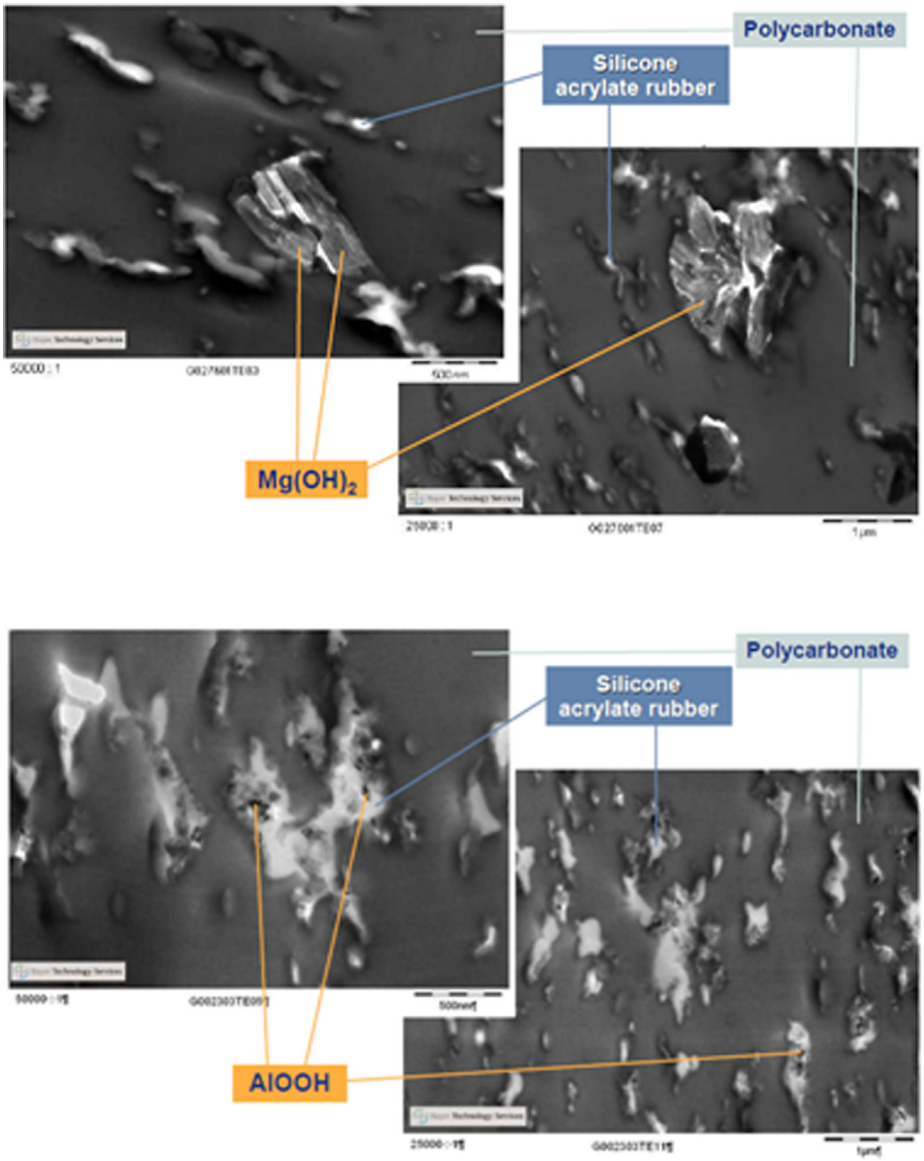

Fig. 7. TEM pictures of PC/SiR/BDP + AlO(OH) and PC/SiR/BDP + $Mg(OH)_2$ (provided by BayerMaterial Science AG).

Please cite this article in press as: Wawrzyn E, et al., Flame-retarded bisphenol A polycarbonate/silicon rubber/bisphenol A bis(diphenyl phosphate): Adding inorganic additives, Polymer Degradation and Stability (2013), http://dx.doi.org/10.1016/j.polymdegradstab.2013.08.006

behaviour in THE. Metal hydroxides worsened the LOI, whereas the UL 94 results remained as good as for PC/SiR/BDP. None inorganic filler showed any influence on BDP's gas phase mode of action; nevertheless, they provide smoke suppression.

3.3. Metal oxides and carbonate

MgO and SiO_2 are thermally stable fillers. They did not decompose within the temperature range investigated in TG (data not shown). Chalk started to decompose endothermically at 650 K, releasing CO_2. The maximum of the mass loss is at 1025 K. The residue was 56 wt.-% (Fig. 1c), corresponding to all $CaCO_3$ transformed into CaO.

Adding MgO, $CaCO_3$ and SiO_2 changed the decomposition of PC/SiR/BDP significantly (Fig. 1c and Table 1). A third decomposition step was observed. PC/SiR/BDP + MgO started to decompose first, at 31 K even before PC/SiR/BDP. Both PC/SiR/BDP + $CaCO_3$ and PC/SiR/BDP + SiO_2, started decomposition around 11 K earlier than PC/SiR/BDP. All the decomposition steps were shifted to lower temperatures compared to PC/SiR/BDP and the mass loss of the first decomposition was around 4 wt.-% lower, indicating fewer interactions between acrylics and PC. PC/SiR/BDP + MgO, PC/SiR/BDP + $CaCO_3$ and PC/SiR/BDP + SiO_2 resulted in residues lower than expected from superimposition. For PC/SiR/BDP + MgO 2.5 wt.-% was lost, for PC/SiR/BDP + $CaCO_3$ 2.3 wt.-% and for PC/SiR/BDP + SiO_2 1.5 wt.-%. Metal oxides and carbonate accelerated the PC/SiR/BDP decomposition and disturbed the cross-linking.

Evolved gas analysis for PC/SiR/BDP + MgO, PC/SiR/BDP + SiO_2 and PC/SiR/BDP + $CaCO_3$ (Fig. 8) showed a clear separation between the decomposition of acrylic components in the first decomposition step, PC decomposition starting in the main decomposition step, and PDMS decomposition in the last decomposition step. Much more phenol derivatives and cyclic siloxanes were released, proving that metallic species promote scission of the PC, BDP and PDMS. The blends with $CaCO_3$ and SiO_2 decreased the amount of acrylates released in comparison to PC/SiR/BDP.

The shifting to lower decomposition temperatures is probably caused by interactions between alkaline metal ions and acidic groups of decomposing PMMA, PBA and PC. Such co-ordination structures were reported to yield tri-dimensional networks and liberation of water as well as CO_2 [33,34] in the case of $CaCO_3$. The ionic interactions at the first decomposition step of PC/SiR/BDP + $CaCO_3$ between acid segments of PBA and calcium carbonate are illustrated in Fig. 9.

The earlier PC decomposition was due to water produced during the first decomposition step and the interaction between metal ions and decomposing PC. Kolbe-Schmitt rearrangement structures form a pendant carboxyl group, at the ortho position to an ether linkage in the main chain. The carboxyl group may also react with the metal oxides. Fig. 10 shows proposed interactions in PC/SiR/BDP + MgO. Analogous interactions have been reported for $CaCO_3$ before [35]. The similar pyrolysis characteristic of PC/SiR/BDP + SiO_2 PC/SiR/BDP + $CaCO_3$ and PC/SiR/BDP + MgO indicated the existence of acid–base interactions also between the SiO_2 surface or silanols and the carbonyl groups of decomposing PBA, PMMA and PC [49]. These decomposition pathways competed with the transesterification reactions between PC and BDP as well as PC and PDMS. The separation of the PC and PDMS decomposition steps for PC/SiR/BDP + MgO, PC/SiR/BDP + $CaCO_3$ and PC/SiR/BDP + SiO_2 ruled out any influence by PC on PDMS decomposition. More cyclic siloxanes were observed in the gas phase (Fig. 8).

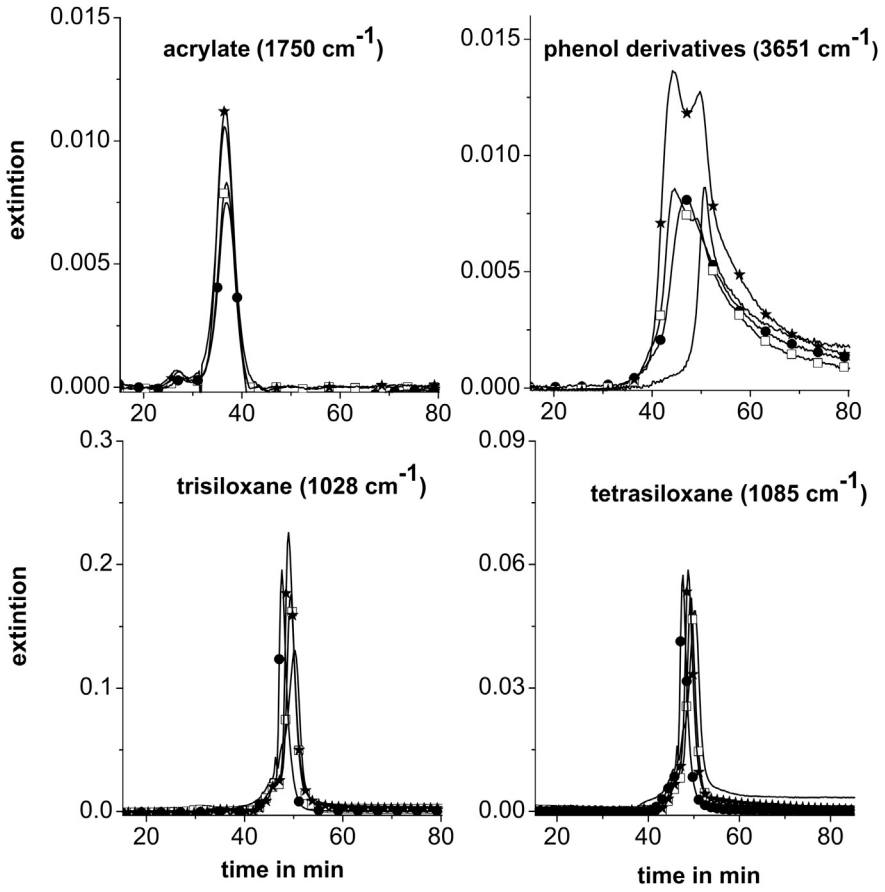

Fig. 8. Pyrolysis product release rates for PC/SiR/BDP + MgO (stars), PC/SiR/BDP + $CaCO_3$ (squares) and PC/SiR/BDP + SiO_2 (circles) compared to PC/SiR/BDP (line).

Please cite this article in press as: Wawrzyn E, et al., Flame-retarded bisphenol A polycarbonate/silicon rubber/bisphenol A bis(diphenyl phosphate): Adding inorganic additives, Polymer Degradation and Stability (2013), http://dx.doi.org/10.1016/j.polymdegradstab.2013.08.006

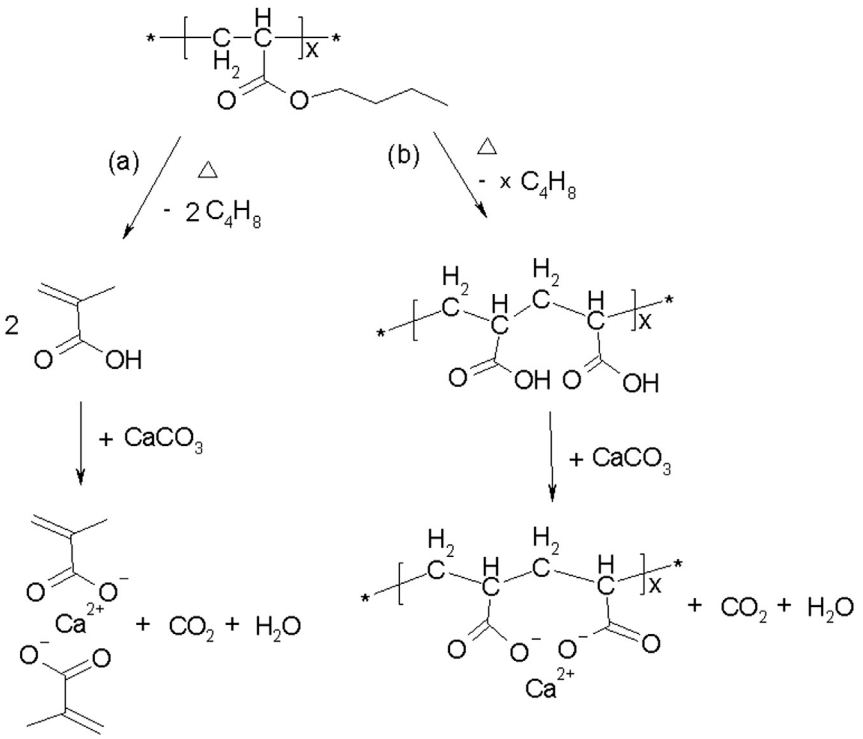

Fig. 9. Ionic interactions between $CaCO_3$ and acidic functions of PBA.

Combining $CaCO_3$ and PDMS in PC/SiR/BDP + $CaCO_3$ caused the decomposing polymer to swell; intumescence occurred. This phenomenon has been reported before for ethylene-acrylate copolymer [35]. At higher temperatures (>850 K) the silicon oxides reacted with CaO to form Ca_2SiO_4 [34,35].

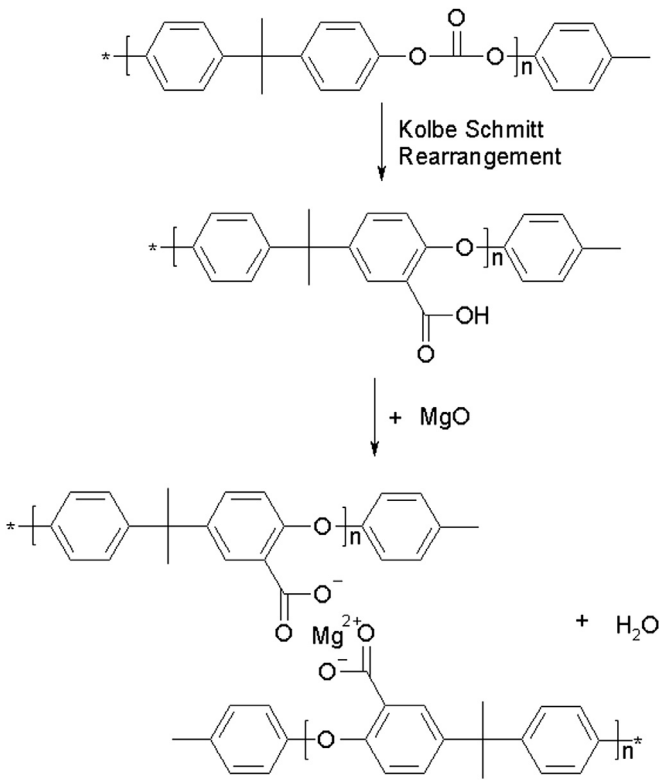

Fig. 10. Ionic interactions between MgO and acidic functions of PC from Kolbe Schmitt rearrangement.

The thermal decomposition pathway in PC/SiR/BDP + MgO, PC/SiR/BDP + $CaCO_3$ and PC/SiR/BDP + SiO_2 was changed considerably. Ionomeric interactions accelerated the PC/SiR/BDP decomposition and competed with the reduction of residue caused by PC-BDP and PC-PDMS cross-linking. The blend with $CaCO_3$ created an intumescent structure during burning. The effect of using silica is also related to silanol groups, which promote the PC and PDMS decomposition [28].

Metal oxides and carbonate worsened the flammability (reaction to small flame) results (Table 2). The worst results were observed for PC/SiR/BDP + $CaCO_3$ when LOI was lowered by nearly a quarter compared to PC/SiR/BDP and yields only HB in UL 94. The reduction for adding MgO and SiO_2 was slightly less in LOI, and PC/SiR/BDP + SiO_2 and PC/SiR/BDP + MgO showed V0 and V1, respectively, for both sample thicknesses in UL 94.

The HRR curve patterns for PC/SiR/BDP + $CaCO_3$, PC/SiR/BDP + SiO_2 and PC/SiR/BDP + MgO were same as for PC/SiR/BDP. PC/SiR/BDP + MgO showed an increased char stability against decomposition. All characteristics such as pHRR, THE, residue, THE/ML are the same. Significant differences occurred only for TCOP/ML Metallic species decreased TCOP/ML in the order: PC/SiR/BDP > PC/SiR/BDP + SiO_2 > PC/SiR/BDP + MgO > PC/SiR/BDP + $CaCO_3$.

PC/SiR/BDP + SiO_2 did not show pronounced accumulation of the inorganic components at the surface of the fire residue. The formation of an inorganic protection layer did not occur, even though the SEM/SEM-EDX investigation identified phase separation between the components (Fig. 11). Unfortunately the clearly different and intumescent residue also obtained for PC/SiR/BDP + $CaCO_3$ did not provide any additional protective effect, since it collapsed during burning (Fig. 12).

3.4. Hydrated metal borates

The characteristic results for decomposition in TG are reported for ZnB, CaB, MgB and their blends with PC/SiR/BDP in Fig. 1d and Table 1. Among the borates investigated, ZnB was the most stable,

Please cite this article in press as: Wawrzyn E, et al., Flame-retarded bisphenol A polycarbonate/silicon rubber/bisphenol A bis(diphenyl phosphate): Adding inorganic additives, Polymer Degradation and Stability (2013), http://dx.doi.org/10.1016/j.polymdegradstab.2013.08.006

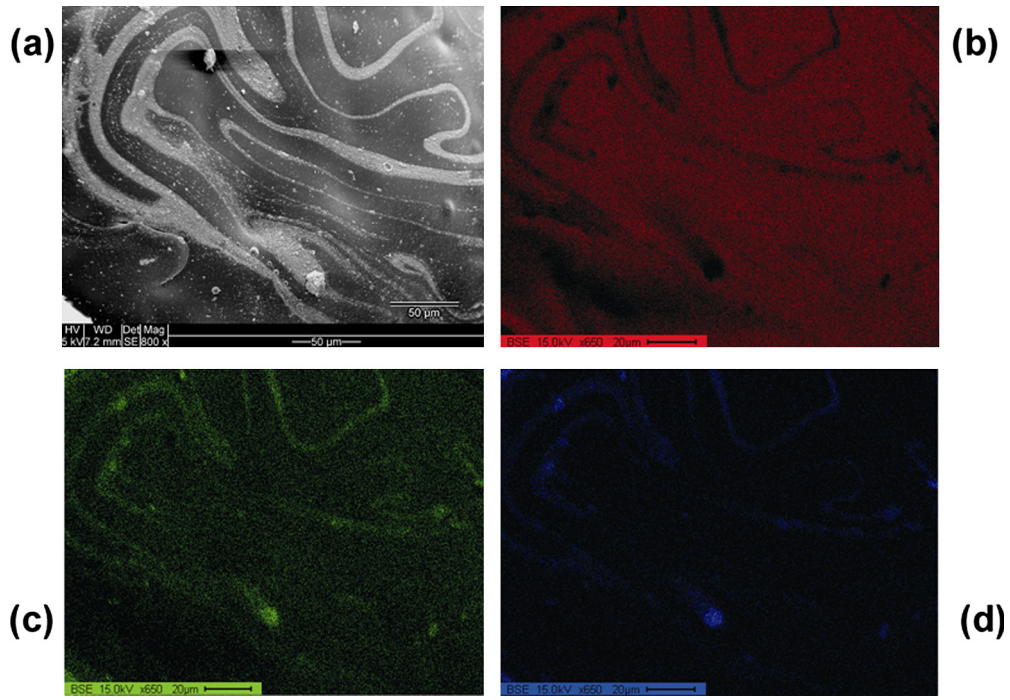

Fig. 11. The dispersion of SiO_2 in fire residue of PC/SiR/BDP + SiO_2; (a) SEM lateral view showing the PC/SiR/BDP + SiO_2 and EDX distribution map of the C element (b), O element (c) and Si element (d).

starting its decomposition at 622 K and decomposing in two steps around 6 wt.-% mass loss with maximum mass loss rates at T_{max} = 630 K and 692 K. The residue was 87.7 wt.-%. The mass loss was attributed to hydrated water. CaB and MgB start to decompose at 274 K. MgB showed two decomposition processes at T_{max} = 374 K and 484 K with a residue of 76 wt.-%. CaB decomposes in three steps (T_{max} = 378 K, 495 K and 697 K) and yields 81 wt.-% residue.

The release of water resulted in slightly earlier decomposition of the blends, but the number of decomposition steps remained unchanged as did the mass loss during the first step. The second mass loss was significantly lower, reflecting the lowered PC content; the residue was increased by the expected ~4 wt.-%. For PC/SiR/BDP + CaB, the blend with the highest water content, the second decomposition step is shifted to temperatures 11 K lower. The product release rates (Fig. 13) showed that adding borates results in an earlier release of cyclic siloxanes. PC/SiR/BDP + CaB releases CO_2 and phenol derivatives slightly earlier than other systems, probably also due to the higher water content. The hydrolysis for all borates enhanced the PC, PDMS and/or BDP decomposition; thus, much more phenol derivatives and cyclic siloxanes were observed in the gas phase.

^{29}Si NMR, ^{11}B NMR and ^{31}P NMR results obtained for the condensed residue of PC/SiR/BDP + ZnB are presented in Fig. 14. Analogous to the PC/SiR/BDP [3,16], signals corresponding to D, T and Q groups appeared in the ^{29}Si MAS NMR spectra, indicating the formation of an amorphous silicate network. This happened for PC/SiR/BDP + ZnB at lower temperatures than for PC/SiR/BDP and is thus consistent with the evolved gas analysis.

The two resonances, at about 0 ppm and between 17 ppm and 5 ppm in the initial ^{11}B NMR spectrum of PC/SiR/BDP + ZnB, mark tetrahedral BO_4 units and the complex BO_3 resonance for highly symmetric BO_3 units where all oxygen atoms are bridging. When temperature increased, the BO_3/BO_4 ratio increased. All of the boron remains in the condensed residue, forming the amorphous borate network. For more than 70 wt.-% mass loss of PC/SiR/BDP + ZnB a novel resonance was monitored at − 5 ppm. Tetragonal borate units were proposed at the border of the amorphous borate network, linked by bridging oxygen to phosphate units. Borate units of ZnB and PDMS did not react with each other, so that separate silicate and borate networks were formed during PC/SiR/BDP + ZnB decomposition.

The ^{31}P NMR spectra of PC/SiR/BDP + ZnB (Fig. 14) reveal decomposition products of BDP with increasing temperature that are quite similar to those observed for PC/SiR/BDP [3,16]. BDP reacts with decomposing PC to form various aromatic phosphate esters during pyrolysis. These phosphates converted to phosphonates at the end of decomposition. Further, a new peak was observed at 3.4 ppm, characteristic for α-zinc phosphate (α-$Zn_3(PO_4)_2$). An interaction between ZnB and BDP became obvious in the condensed phase.

Adding ZnB, CaB and MgB influenced the thermal decomposition of PC/SiR/BDP. The hydrated borates released water, which triggered enhanced PC, BDP and PDMS decomposition. Thus more phenolic derivatives and cyclic siloxanes were observed in the gas phase, accompanied by less cross-linking between PC, PDMS and BDP. Nevertheless, borates contributed to the residue due to the formation of inorganics. A borate network (BO_3/BO_4 ratio shifted towards BO_3) and metal phosphates were proven unambiguously by NMR, whereas no mixed silicate borate network was observed. The limited formation of metal phosphates and BPO_4 resulted from the interaction between BDP and borates. ZnB, MgB and CaB in PC/SiR/BDP form thermal stable, boron-based glass, probably protecting the carbonaceous char or improving its properties [38,50].

The use of ZnB, CaB and MgB in PC/SiR/BDP showed slightly better flammability (reaction to small flame) than PC/SiR/BDP (Table 2). The LOI tended to increase. Among all investigated blends containing borates, PC/SiR/BDP + CaB showed the highest LOI and V0 classification for both investigated thicknesses.

The HRR of PC/SiR/BDP + ZnB, PC/SiR/BDP + CaB and PC/SiR/BDP + MgB were characterized by the same patterns as discussed

Please cite this article in press as: Wawrzyn E, et al., Flame-retarded bisphenol A polycarbonate/silicon rubber/bisphenol A bis(diphenyl phosphate): Adding inorganic additives, Polymer Degradation and Stability (2013), http://dx.doi.org/10.1016/j.polymdegradstab.2013.08.006

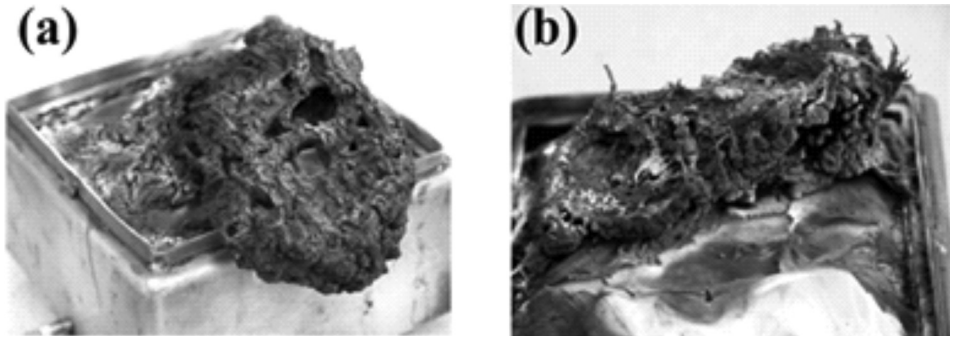

Fig. 12. Fire residues of (a) PC/SiR/BDP and (b) PC/SiR/BDP + $CaCO_3$ under 50 kW m^{-2} irradiation.

for PC/SiR/BDP. The THE is not influenced within the limits of uncertainty. The pHRR seemed to be the same for 35 kW m^{-2} and showed a tendency to reduction for the higher irradiations 50 kW m^{-2} and 70 kW m^{-2}. The residue was hardly changed; only PC/SiR/BDP + ZnB showed significantly higher residue. Zinc is more effective than calcium and magnesium in terms of charring, most probable because it is the much stronger Lewis acid.

THE/ML was hardly influenced for the lower heat flux 35 kW m^{-2}, but decreased for PC/SiR/BDP + MgB and PC/SiR/BDP + ZnB at the higher heat fluxes (50 kW m^{-2} and 70 kW m^{-2}). Indeed, combining BDP and ZnB resulted in switching off the gas-phase action of BDP as has been reported before for a comparable system [37,51]. Adding ZnB, CaB and MgB decreased CO production and smoke production. The effect is always the highest for PC/SiR/BDP + ZnB.

Adding different borates, ZnB, CaB and MgB, to PC/SiR/BDP tended to improve the reaction to small flame as it is tested in LOI and UL 94, even though the effect is small. Further, they harbour the potential to improve charring and function as a smoke suppressant. The reactions seemed to depend on the applied heat flux and were always clearly stronger for ZnB. At higher heat fluxes the reaction between BDP and ZnB increased the phosphorous remaining in the condensed phase by forming metal phosphates and borophosphates. The gas-phase action vanished, whereas a glassy coating improved the char properties.

4. Conclusion

Various inorganic additives were added to PC/SiR/BDP in order to improve the flame retardancy of the blend. Based on the

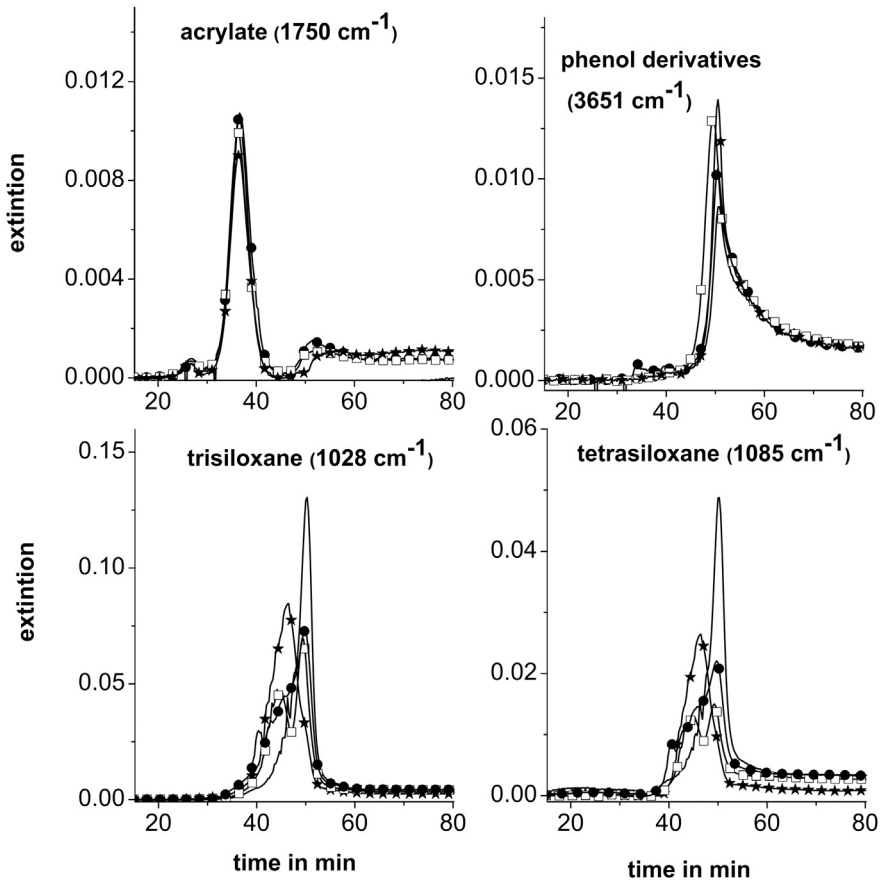

Fig. 13. Pyrolysis product release rates (TG-FTIR) for PC/SiR/BDP + ZnB (circles), PC/SiR/BDP + MgB (stars) and PC/SiR/BDP + CaB (squares) compared to PC/SiR/BDP (line).

Please cite this article in press as: Wawrzyn E, et al., Flame-retarded bisphenol A polycarbonate/silicon rubber/bisphenol A bis(diphenyl phosphate): Adding inorganic additives, Polymer Degradation and Stability (2013), http://dx.doi.org/10.1016/j.polymdegradstab.2013.08.006

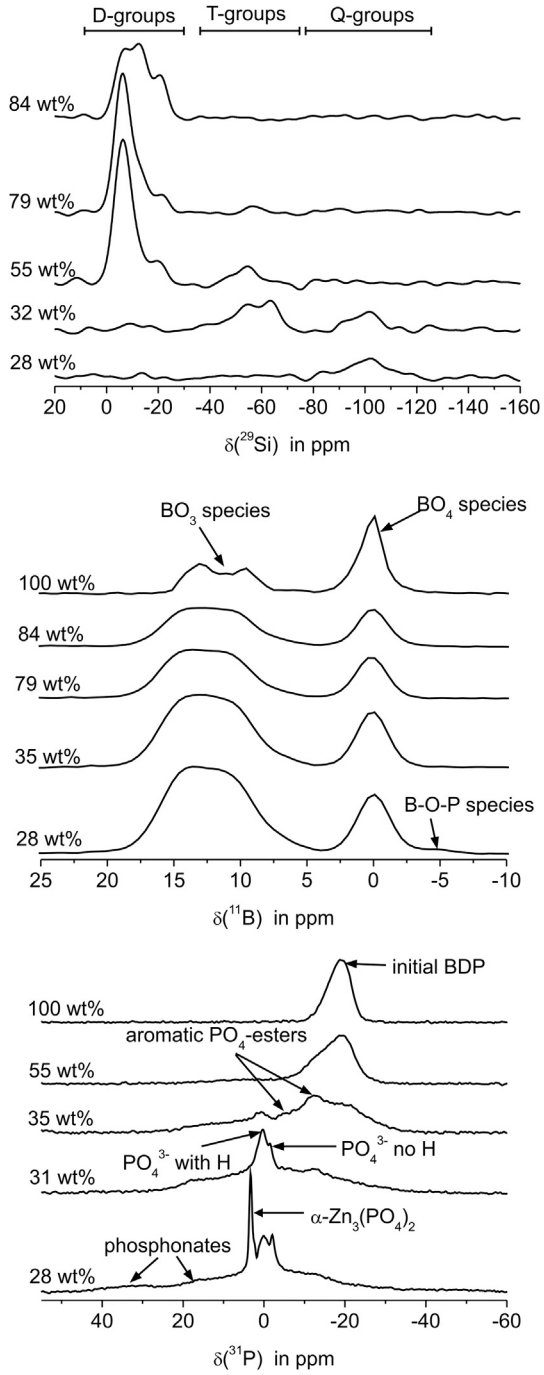

Fig. 14. ^{29}Si NMR, ^{11}B NMR and ^{31}P NMR on solid residues of PC/SiR/BDP + ZnB.

chemical structure of the fillers used, they were sorted into four different groups: layered materials, metal hydroxides, metal oxides and carbonate as well as metal borates. Their pyrolysis, reaction to small flame and fire behaviour were investigated; additional experiments such as rheology and NMR were used to underline the structure-property-relationships.

Among the layered materials added, talc was an inert filler with respect to pyrolysis, whereas organically modified montmorillonite enhanced the decomposition of PC/SiR/BDP. The forced-flaming behaviour of both PC/SiR/BDP + talc and PC/SiR/BDP + LS indicated a mechanical reinforcement of the char, somewhat decreasing the pHRR. Both LS and talc enhanced the flow limit; LS worked as a plasticiser at higher shear rates. The LOI were reduced compared to PC/SiR/BDP. Adding LS in PC/SiR/BDP + LS deteriorated the UL 94 classification to HB; PC/SiR/BDP + talc showed V-0 as PC/SiR/BDP. The PC/SiR/BDP + LS nanocomposite seemed to worsen performance. Using PC/SiR/BDP + talc microcomposite is proposed to be of interest, whereby in practise adding talc is also motivated by its potential for mechanical reinforcement.

When comparing the addition of two different types of metal hydrates, AlO(OH) nano-particle and $Mg(OH)_2$ micro-particle, the pyrolysis strongly depends on their dispersion and location within PC/SiR/BDP. The AlO(OH) was concluded to be embedded in SiR and thus behaved as an inert filler, whereas the $Mg(OH)_2$ was dispersed within the PC matrix, inducing additional hydrolysis of PC at lower decomposition temperatures. This hydrolysis disturbed the condensed phase action of BDP and led to less char formation. Both additives worked as smoke suppressants and reduced the effective carbon monoxide production. The pHRR tended to decrease for higher irradiations. Both AlO(OH) and $Mg(OH)_2$ worsen the LOI, but UL 94 results remained V-0 like PC/SiR/BDP. Additional hydrolysis is always a challenge to overcome when using metal hydrates in PC. Using nano-particles as phase selective fillers seemed to be an interesting route to achieve this in PC/SiR blends.

The effect of adding metal oxides and carbonate, namely MgO, $CaCO_3$ and SiO_2, was investigated. These additives change the decomposition pathways of PC/SiR/BDP crucially. The interactions with acidic groups of PMMA, PBA and PC as well as the formation of inorganic phosphates ultimately worsened the fire performance of PC/SiR/BDP. Adding MgO did not enhance the formation of carbonaceous char. $CaCO_3$ harboured the potential to intumescence, but this phenomenon was not exploited due to an early collapse of the char structure during combustion. Adding SiO_2 did not result in any noticeable improvement of the residue. Adding MgO, $CaCO_3$ and SiO_2 to PC/SiR/BDP clearly deteriorated the LOI. Nevertheless, PC/SiR/BDP + SiO_2 still showed V-0 classification; PC/SiR/BDP + MgO shows V1; and PC/SiR/BDP + $CaCO_3$ achieved only HB.

When hydrated metal borates were added, CaB, MgB and ZnB to some extent enhanced the early decomposition of PC/SiR/BDP due to the liberation of water. Reaction with BDP to form metal and borophosphates changed the condensed-phase action and decreased the amount of phosphorus released for flame inhibition in fire scenarios with higher heat fluxes. A vitreous layer tended to decrease the pHRR. Smoke suppression was observed for ZnB and for CaB in the more fully developed fire scenario. Adding ZnB, MgB and CaB slightly increased the LOI of PC/SiR/BDP and yielded the best UL 94 classification, V0. ZnB always performed better than MgB and CaB.

PC/SiR/BDP is a highly sensitive system with respect to chemical interactions. The interactions between PC, SiR and BDP are already complex and the use of BDP in PC blends is believed to be a superior approach based on an adjusted balance between a major gas-phase and minor condensed-phase flame retardancy action by BDP. Testing several inorganic fillers, it seems that it is much easier to disturb the flame retardancy in PC/SiR/BDP than to enhance it. Nevertheless, comparing the results of different inorganic fillers in four different groups delivered some valuable hints about how to proceed. The PC/SiR/BDP + talc micro-composite approach works much better than the PC/SiR/BDP + LS nanocomposite. AlO(OH) phase-selective nanocomposite was proposed to harbour potential for future advances. The changes in pyrolysis by metal oxides and carbonate may be less promising in PC than is known for other technical polymers. Performance of ZnB was superior to that of other borates, so that adding ZnB to PC/SiR/BDP succeeded in improving fire performance.

The comprehensive study using systematic comparisons of different inorganic additives offers valuable guidelines for the future development of flame-retarded multi-component PC blends.

Please cite this article in press as: Wawrzyn E, et al., Flame-retarded bisphenol A polycarbonate/silicon rubber/bisphenol A bis(diphenyl phosphate): Adding inorganic additives, Polymer Degradation and Stability (2013), http://dx.doi.org/10.1016/j.polymdegradstab.2013.08.006

Acknowledgements

The support received from BayerMaterial Science AG, in particular from V. Taschner, M. Jung, T. Eckel and D. Wittmann, is gratefully acknowledged. We also thank U. Braun for fruitful discussion and H. Bahr as well as H. Seefeldt, F. Kempel and E. Dümichen for their help with recording the measurements.

References

[1] Perret B, Schartel B. The effect of different impact modifiers in halogen-free flame retarded polycarbonate blends – I. Pyrolysis. Polym Degrad Stab 2009;94:2194–203.
[2] Perret B, Schartel B. The effect of different impact modifiers in halogen-free flame retarded polycarbonate blends – I. Fire behaviour. Polym Degrad Stab 2009;94:2204–12.
[3] Wawrzyn E, Schartel B, Seefeldt H, Karrasch A, Jäger C. What reacts with what in bisphenol A polycarbonate/silicon rubber/bisphenol A bis(diphenyl phosphate) during pyrolysis and fire behavior? Ind End Chem Res 2012;51:1244–55.
[4] Levchik SV, Weil ED. Developments in phosphorus flame retardants. In: Horrocks A, Price D, editors. Advances in fire retardant materials. Cambridge: Woodhead Publishing; 2008. p. 42–3.
[5] Granzow A. Flame retardation by phosphorus compounds. Acc Chem Res 1978;11:177–83.
[6] Levchik SV, Weil ED. A review of recent progress in phosphorus-based flame retardants. J Fire Sci 2006;24:345–64.
[7] Levchik SV, Weil ED. Flame retardants in commercial use or in advanced development in polycarbonates and polycarbonate blends. J Fire Sci 2006;24:137–51.
[8] Hastie JW. Molecular basis of flame inhibition. J Res Nat Bur Stand Sect A Phys Chem 1973;77A:733–54.
[9] Despinasse MC, Schartel B. Aryl phosphate–aryl phosphate synergy in flame-retarded bisphenol A polycarbonate/acrylonitrile-butadiene-styrene. Thermochim Act 2013;563:51–61.
[10] Pawlowski KH, Schartel B. Flame retardancy mechanisms of triphenyl phosphate, resorcinol bis(diphenyl phosphate) and bisphenol bis(diphenyl phopshate) in polycarbonate/acrylonitrile-butadiene-styrene blends. Polym Int 2007;56:1404–14.
[11] Schartel B. Phosphorus-based flame retardancy mechanisms – old hat or starting point for future development? Materials 2010;3:4710–45.
[12] Murashko EA, Levchik GF, Levchik SV, Bright DA, Dashevsky S. Fire-retardant action of resorcinol bis(diphenyl phosphate) in PC-ABS blend. II. Reactions in the condensed phase. J Appl Polym Sci 1999;71:1863–72.
[13] Perret B, Pawlowski KH, Schartel B. Fire retardancy mechanisms of arylphosphates in polycarbonate (PC) and PC/acrylinitrile-butadiene-styrene: the key role of decomposition temperature. J Therm Anal Calorim 2009;97:949–58.
[14] Despinasse MC, Schartel B. Influence of the structure of arylphosphates on the flame retardancy of polycarbonate/acrylonitrile-butadiene-styrene. Polym Degrad Stab 2012;97:2479–626.
[15] Karrasch A, Wawrzyn E, Schartel B, Jäger C. Solid-state NMR on thermal and fire residues of bisphenol A polycarbonate/silicone acrylate rubber/bisphenol A bis(diphenyl-phosphate)/(PC/SiR/BDP) and PC/SiR/BDP/zinc borate (PC/SiR/BDP/ZnB); part I: PC charring and the impact of BDP and ZnB. Polym Degrad Stab 2010;95:2525–33.
[16] Karrasch A, Wawrzyn E, Schartel B, Jäger C. Solid-state NMR on thermal and fire residues of bisphenol A polycarbonate/silicone acrylate rubber/bisphenol A bis(diphenyl-phosphate)/(PC/SiR/BDP) and PC/SiR/BDP/zinc borate (PC/SiR/BDP/ZnB); part II: the influence of SiR. Polym Degrad Stab 2010;95:2534–40.
[17] Weil ED. Synergists, adjuvants and antagonists in flame retardant systems. In: Grand AF, Wilkie CA, editors. Fire retardancy of polymeric materials. New York: Marcel Dekker Inc; 2000. p. 115–45.
[18] Gilman JW, Kashiwagi T, Lichtenbahn JD. Nanocomposites: a revolutionary new flame retardant approach. SAMPLE J 1997;33:40–6.
[19] Schartel B, Bartholmai M, Knoll U. Some comments on the main fire retardancy mechanisms in polymer nanocomposites. Polym Adv Technol 2006;17:772–7.
[20] Bartholmai M, Schartel B. Layered silicate polymer nanocomposites: new approach or illusion for fire retardancy? Investigations on the potential and on the tasks using a model system. Polym Adv Technol 2004;15:355–64.
[21] Horn WE. Inorganic hydroxides and hydrocarbonates: their function and use as flame-retardant additives. In: Grand AF, Wilkie CA, editors. Fire retardancy of polymeric materials. New York: Marcel Dekker Inc; 2000. p. 285–352.
[22] Hornsby PR. Fire retardant fillers for polymers. Int Mater Rev 2001;46:199–210.
[23] Braun U, Schartel B. Flame retardant mechanisms of red phosphorus and magnesium hydroxide in high impact polystyrene. Macromol Chem Phys 2004;205:2185–96.
[24] Pawlowski KH, Schartel B. Flame retardancy mechanisms of arylphosphastes in combination with boehmite in bisphenol A polycarbonate/acrylonitrile-butadiene-styrene blends. Polym Degrad Stab 2008;93:657–67.
[25] Gallo E, Braun U, Schartel B, Russo P, Acierno D. Halogen-free flame retarded poly(butylene terephthalate) (PBT) using metal oxides/PBT nanocomposites in combination with aluminium phosphinate. Polym Degrad Stab 2009;94:1245–53.
[26] Laachachi A, Cochez M, Leroy E, Ferriol M, Lopez-Cuesta JM. Fire retardant systems in poly(methyl methacrylate): interactions between metal oxide nanoparticles and phosphinates. Polym Degrad Stab 2007;92:61–9.
[27] Gallo E, Schartel B, Acierno D, Russo P. Flame retardant biocomposites: synergism between phosphinate and nanometric metal oxides. Eur Polym J 2011;47:1390–401.
[28] Kashiwagi T, Gilamn JW, Butler KM, Harris RH, Shields JR, Asano A. Flame retardant mechanism of silica gel/silica. Fire Mater 2000;24:277–89.
[29] Gallo E, Schartel B, Schmaucks G, von der Ehe K, Böhning M. The effect of well-dispersed amorphous silicon dioxide in flame-retarded styrene butadiene rubber. Plast Rubber Compos 2013;42:34–42.
[30] Garcia N, Corrales T, Guzman J, Tiemblo P. Understanding the role of nano-silica particle surfaces in the thermal degradation of nanosilica-poly(methyl methacrylate) solution-blended nanocomposites: from low to high silica concentration. Polym Degrad Stab 2007;92:635–43.
[31] Schmaucks G, Roszinski JO. European Patent, EP 1824917.
[32] Schartel B, Schmaucks G, Roszinski JO. Norway Patent, NO 20084323.
[33] Karlsson L, Lundgren A, Jungqvist J, Hjertberg T. Influence of melt behaviour on the flame retardant properties of ethylene copolymers modified with calcium carbonate and silicone elastomer. Polym Degrad Stab 2009;94:527–32.
[34] Krämer RH, Raza MA, Gedde UW. Degradation of poly(ethylene-co-methacrylic acid) - calcium carbonate nanocomposites. Polym Degrad Stab 2007;92:1795–802.
[35] Hermansson A, Hjertberg T, Sultan B- A. The flame retardant mechanism of polyolefins modified with chalk and silicone elastomer. Fire Mater 2003;27:51–70.
[36] Hermansson A, Hjertberg T, Sultan B- A. Linking the flame retardant mechanisms of an ethylene-acrylate copolymer, chalk and silicone elastomer system with its intumescent behaviour. Fire Mater 2005;29:407–26.
[37] Pawlowski KH, Schartel B, Fischera MA, Jäger C. Flame retardancy mechanisms of bisphenol A bis(diphenyl phosphate) in combination with zinc borate in bisphenol A polycarbonate/acrylonitrile-butadiene-styrene blends. Thermochim Acta 2010;498:92–9.
[38] Shen KK, Kochesfahani S, Jouffret F. Zinc borates as multifunctional polymer additives. Polym Adv Technol 2008;19:469–74.
[39] Bourbigot S, Le Bras M, Leeuwendal R, Shen KK, Schubert D. Recent advances in the use of zinc borates in flame retardancy of EVA. Polym Degrad Stab 1999;64:419–25.
[40] Levchik GF, Levchik SV, Selevich AF, Lesnikovich AI. The effect of ammonium pentaborate on combustion and thermal decomposition of polyamide 6. Vesti Akad Nauk Belarusi Ser Khim Nauk 1995;3:34–9.
[41] Ozawa T. A new method of analyzing thermogravimetric data. Bull Chem Soc Jpn 1965;38:1881–6.
[42] Sturm H, Schartel B, Weiß A, Braun U. SEM/EDX: advanced investigation of structured fire residues and residue formation. Polym Test 2012;31:606–19.
[43] Schartel B, Hull TR. Development of the cone calorimeter – a bench scale heat release rate apparatus based on oxygen consumption. Fire Mater 2007;31:327–54.
[44] Sinha Ray S, Okamoto M. Polymer/layered silicate nanocomposites: a review from preparation to processing. Prog Polym Sci 2003;28:1539–641.
[45] Schartel B, Pötschke P, Knoll U, Abdel-Goad M. Fire behaviour of polyamide 6/multiwall carbon nanotube nanocomposites. Eur Polym J 2005;41:1061–70.
[46] Dittrich B, Wartig K-A, Hofmann D, Mülhaupt R, Schartel B. Carbon black, multiwall carbon nanotubes, expanded graphite and functionalized graphene flame retarded polypropylene nanocomposites. Polym Adv Technol 2013[in press].
[47] Reimschuessel HK, Shalaby SW, Pearce EM. On the oxygen index of nylon 6. J Fire Flammability 1973;4:299–308.
[48] Schartel B, Richter KH, Böhning M. Synergistic use of talc in halogen-free flame retarded polycarbonate/acrylonitrile-butadiene-styrene blends. In: Morgan AB, Wilkie CA, Nelson GL, editors. fire and polymers VI: new advances in flame retardant chemistry and science. Washington: ACS; 2012. p. 15–36. ACS symposium series 1118, chap. 2.
[49] Grohens Y, Auger M, Prud'homme R, Schults J. Adsorption of stereoregular poly(methyl methacrylate) on alumina: spectroscopic analysis. J Polym Sci Part B Polym Phys 1999;37:2985–95.
[50] Bellayer S, Tavard E, Duquesne S, Piechazyk A, Bourbigot S. Mechanism of intumescence of a polyethylene/calcium carbonate/stearic acid system. Polym Degrad Stab 2009;94:797–803.
[51] Schartel B, Pawlowski KH, Lyon RE. Pyrolysis combustion flow calorimeter: A tool to assess flame retarded PC/ABS materials? Thermochim Act 2007;462:1–14.

Please cite this article in press as: Wawrzyn E, et al., Flame-retarded bisphenol A polycarbonate/silicon rubber/bisphenol A bis(diphenyl phosphate): Adding inorganic additives, Polymer Degradation and Stability (2013), http://dx.doi.org/10.1016/j.polymdegradstab.2013.08.006